

Reutilization of waste inert glass from the disposal of polluted dredging spoils by the obtainment of ceramic products for tiles applications

G. BRUSATIN, E. BERNARDO

Dipartimento di Ingegneria Meccanica—Settore Materiali, Università di Padova, Via Marzolo 9, 35131 Padova, Italia

F. ANDREOLA, L. BARBIERI, I. LANCELLOTTI

Dipartimento di Ingegneria dei Materiali e dell'Ambiente, Università di Modena e Reggio Emilia, Via Vignolese 905, 41100 Modena, Italia

S. HREGLICH

Stazione Sperimentale del Vetro, Via Briati 10, 30121 Murano (Ve), Italy

The vitrification treatment has been successfully exploited as a solution for the disposal of polluted dredging spoils from the industrial area close to the Venice Lagoon. The addition of 20% by wt. of glass cullet to the calcined sediments in the vitrification batch provides a suitable chemical composition for the production of an inert glass, despite the compositional variations of the sediments. The obtained waste glass, after being finely ground, has been employed (i) as a raw material for the manufacture of sintered glass-ceramics, by cold pressing and single-step sintering at about 940°C, and (ii) as sintering additive (the maximum addition being 10% by wt.) for the manufacture of traditional red single firing ceramic tiles, with a maximum firing temperature of 1186°C. Both applications have proved to be promising: in the first case, the sintered glass ceramic product exhibits notable mechanical properties (bending strength > 130 MPa, HV ≈ 6.5 GPa); in the second case, the addition of waste glass does not modify substantially the investigated physical and mechanical properties of the traditional product (water absorption, linear shrinkage, bending strength, planarity).

© 2005 Springer Science + Business Media, Inc.

1. Introduction

A solution for encapsulating and making inert various types of wastes (i.e. industrial, contaminated sediments, ashes from municipal waste incinerators) has been successfully identified in the vitrification process [1]. This technology, often employed by correcting the waste composition with inert glass cullet to achieve suitable final durability characteristics, could provide in the future years large amount of glassy materials. The composition of this kind of glass is generally rich in heavy metal oxides normally absent, or present in negligible amount, in the glass used for main commercial applications (bottles, windows, . . .). For this reason, most of the glasses obtained by the vitrification treatment of wastes are consequently stored in landfills. Since the hazardous substances are perfectly immobilized in the glass network (in the case of metals, in the form of the related oxides) or thermally destroyed during the process (in the case of organic pollutants) [1–10], the vitrification technology makes it possible to reuse the

obtained glass in the production of ceramics for building applications, where the problems of low purity and aesthetic aspect of these glasses can be overcome. With the aim of producing ceramics for the building industry, it was often evidenced in the literature the possibility of using glass from the vitrification treatment of wastes in the manufacture of glass ceramic materials [11, 12]. Such solution often exploits the relatively easy tendency to crystallize of such glasses: in fact, a frequent characteristic of glasses obtained from wastes is the presence of Ca, Al and Mg oxides and oxides deriving from the specific waste like Fe, Zn, Cu. . . [8, 13].

In this work the reutilization of a glass obtained from the vitrification of the sediments of an industrial area close to the Venice lagoon is discussed; these are known to be contaminated by several heavy metals and organic pollutants [1, 9]. In this case the composition of dredging spoils was suitable for a direct vitrification at relatively low temperatures, yielding an inert product.

The feasibility of preparing ceramic products was demonstrated for tiles applications (i) from glass from the vitrification treatment of contaminated sediments, leading to the development of sintered glass-ceramics, and (ii) by correcting with different amounts of the same glass the composition of an ordinary industrial ceramic body. In the first case the well-known phenomenon of sinter-crystallization of glasses was exploited as it is currently reported for waste glasses [6, 14] (thanks to the fact that the glass surface is a preferred site for crystallization, powdered glass is easier to devitrify than bulk glass with the same composition) [15, 16]. As is generally observed, in the present investigation the fine granulometry and the cold-pressing of the glass powders led to high densification and remarkable mechanical properties of the final product. In the second case, notwithstanding the amount of glass from wastes is limited, the industrial impact is thought to be very promising, since substantial modifications of the currently employed processing routes are not needed and the overall physical and mechanical properties of the newly developed fired ceramics are comparable to those of traditional products.

2. Experimental

2.1. Preparation of the ceramic materials

The vitrification of the excavated dredging spoils has been described elsewhere [9, 10]. The obtained waste glass ($G = 80\%$ calcined sediments, 20% soda-lime glass cullet) was used to obtain sintered glass-ceramics and several ceramic mixtures, by adding it to a traditional ceramic body (CMG0).

In order to obtain sintered glass-ceramics (SC), powders of (G) waste glass, crushed to a dimension $<38 \mu\text{m}$, were cold-pressed in a steel die (with a rectangular section of $50 \times 34 \text{ mm}$) by using a hydraulic press operating at 40 MPa . The pressed samples were crystallized by holding for 5 h at about 940°C , without the addition of any nucleating agent. The firing temperature has been chosen on the basis of thermal analysis data.

The density of the sintered glass-ceramic (SC) was measured by the Archimedes' principle. At least ten fragments were analysed.

Different ceramic mixtures (CM) have been prepared by adding 2.5 , 5.0 and 10 wt\% of G powder to a traditional red single firing ceramic body to obtain ceramic tiles. The two raw materials were dry mixed obtaining the following compositions: CMG0 (standard, i.e. tile constituted by ceramic body only), CMG2.5, CMG5 and CMG10 with 2.5 , 5 and 10 parts of G frit, respectively. For each mixture cylindrical tiles (40 mm of diameter and 5 mm of thickness of the green sample) were formed by cold pressing, dried and finally fired in an industrial kiln for single firing at the maximum temperature of 1186°C for about 34 min in order to simulate the industrial conditions.

The chemical compositions of G and CMG0 were measured by Inductively Coupled Plasma (ICP Varian Liberty 200) and they are reported in Table I.

TABLE I Chemical analysis (oxide%) of SG glass and ceramic body

	SiO ₂	Al ₂ O ₃	CaO	MgO	Na ₂ O	K ₂ O	Fe ₂ O ₃	TiO ₂	LOI
G inert glass	46.08	12.55	20	6.3	3.04	2.8	6.24	0.72	–
CMG0 ceramic body	64.96	15.55	1.64	1.17	1.70	1.83	4.20	0.52	8.96

2.2. Characterization of the ceramic materials

The crystalline structure of the obtained ceramic materials was investigated by powder X-ray diffraction analysis (XRD, Philips PW 3710) and Scanning Electron Microscopy (Philips SEM XL 40) equipped with energy dispersive X-ray analysis (EDAX PV 9900) performed on the polished ceramic materials either after HF attack ($5\% \text{ vol HF}$ solution, 2 min lasting exposure) or on fresh fractured samples, depending on the kind of sample. The mechanical properties of the final glass and ceramics materials were investigated by measuring the microhardness (Digital Micro Hardness Tester Matsuzawa DMH 2) on polished surfaces, the Young's modulus by the acoustic-resonance method [17] (Grindo Sonic MK5 instrument) and the bending strength (Instron 1121 UTM machine). In the case of the sintered glass-ceramic product the bending strength test was conducted on polished samples with dimensions of $3 \times 2 \times 42 \text{ mm}^3$ in a four-point configuration (upper span of 30 mm and inner span of 8 mm); in the case of the fired ceramics the test was conducted on polished samples with dimensions of $4 \times 1.5 \times 30 \text{ mm}^3$ in a three-point configuration (span of 28 mm).

A fracture resistance analysis was performed on the sintered glass-ceramics by means of Vickers' indentation. It is well known that at low loads Vickers' microhardness data are recorded, while at higher loads indentation fracture toughness can be determined, by measuring the length of the cracks emanating from the corners of the Vickers' indents, following the equation [18]:

$$K_{IC} = \xi(E/H)^{0.5}(P/c^{1.5})$$

where E is the elastic modulus, H is the Vickers' hardness, c is the crack length, P is the applied load, ξ is a calibration factor ($\xi = 0.016 \pm 0.004$). In the present investigation the microhardness was measured by applying a load of 500 g , while the fracture toughness was evaluated by applying a load of 3000 g , in order to cause the formation of a well defined crack pattern at the corners of the indent, essential for the equation to be valid.

For the fired ceramic samples, water absorption (WA%) and linear shrinkage (LS%) were measured in order to check the compactness degree due to the sintering process. Measurements with the Hg porosimeter were carried out by Autopore 1215-II (Micromeritics) on the dried sample pieces sized about $4\text{--}5 \text{ mm}$. Porosity was evaluated using the set-time equilibrium (10 s) mode between pressure limits of 3.4 KPa and 414 MPa .

The diameter pore range measured is between 360–0.003 μm .

3. Results and discussion

3.1. Sintered glass-ceramics

The composition of the *G* glass, obtained after vitrification of the dredging spoils, and of the standard ceramic body used in these experiments are reported in Table I.

Sintered ceramics, SC, were made by pressing glass powders and undergoing them to a densification treatment at $T = 937^\circ\text{C}$; the density of the sintered samples increases with the time treatment and reaches a final value of 2.85 g cm^{-3} after 5h treatment. This density is higher with respect to the starting *G* glass (2.80 g cm^{-3}). For comparison, a small size glass ceramics sample can be obtained from the bulk glass after a thermal treatment of at least 24 h at the crystallization temperature (937°C), with a final density of 2.81 g cm^{-3} .

XRD patterns of the SC after 5 h treatment, *G* glass and glass ceramic obtained from bulk treatment for 24 h are reported in Fig. 1. Diopside $\text{Ca}(\text{Mg,Fe,Al})(\text{Si,Al})_2\text{O}_6$ and gehlenite $\text{Ca}_2\text{Al}(\text{Si,Al})_2\text{O}_7$ are the main revealed crystalline phases. From density data and XRD patterns it can be observed that the sintering is very effective to get a dense material in a relatively short thermal treatment time, if compared to that necessary for bulk glass crystallization.

The proposed densification mechanism is a simultaneous viscous phase sintering and crystallization of the solid powder. The viscous phase sintering is known to produce good densification of the green body, with a low residual porosity degree. On the other hand, the powder crystallization is completed in a relatively short time because the nucleation/crystallization phenomenon was found to begin on the surface; in the case of fine powders the high specific surface allows a very effective crystallization process.

Fig. 2 shows the scanning electron microscopy of the glass-ceramic SC. The sample was previously subject to a hydrofluoric acid etching on a polished surface. Since the acid removed the residual glass phase, very small crystals can be observed, with dimensions $<0.5 \mu\text{m}$.

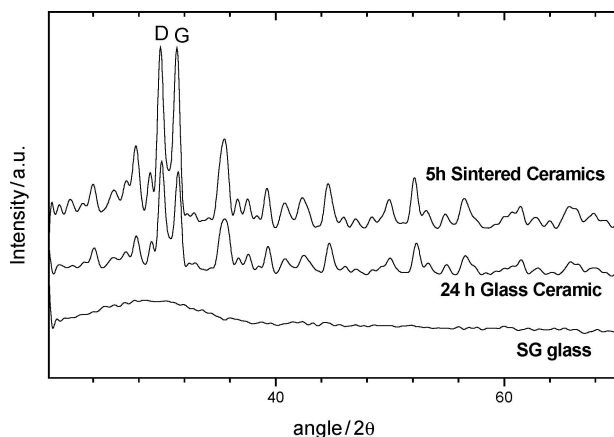


Figure 1 Comparison between the XRD patterns of the SG glass and the CG glass-ceramic.

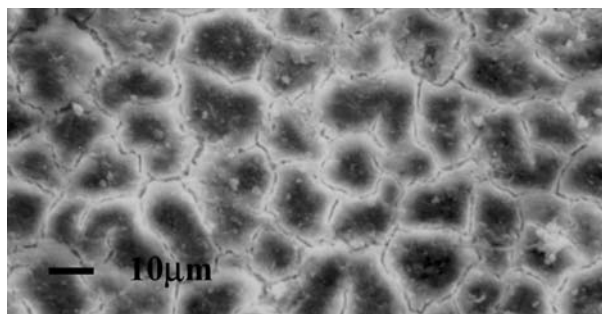


Figure 2 Scanning electron microscopy of the SC sample.

The number of crystals suggests that a high crystallinity degree is achieved.

The occurrence of high densification and high crystallinity is accompanied by notably good mechanical properties, which are summarized in Table II: after a 5 h thermal treatment the sintered glass-ceramic samples exhibit a Vickers' microhardness of 6.5 GPa and a bending strength of about 140 MPa. Such bending strength value far exceeds the data reported for traditional porcelain stoneware ($>50 \text{ MPa}$ [19]). The fracture toughness value is also far beyond the typical values reported for glasses (more than a three-fold increase), and it is remarkable when compared to analogous data for glass-ceramics [20]. Such mechanical properties are believed to be due to the high densification degree, the high crystallinity and the small crystal dimensions (which are particularly profitable to the fracture resistance and hardness).

The high densification determines a relevant linear shrinkage (15%), during the sintering step, which does not compromise the planarity of the final product at all. Also the measured water absorption of the sinter-crystallized sample is remarkable, being lower than 0.1%.

3.2. Fired ceramics

To investigate an alternative tile production process, more suitable for a realistic industrial application, the introduction of relatively small quantities of vitrified sediments in an industrial ceramic body was investigated, making it possible to vary only slightly the usual industrial process.

The X-ray patterns of the fired ceramic mixtures (Fig. 3) revealed, respect to the CMG0, a slight decrease of the quartz peak (main crystalline phase) and an increase of the anorthite ($\text{CaO}\cdot\text{Al}_2\text{O}_3\cdot 2\text{SiO}_2$) content directly proportional to the SG powder introduced, with the constant presence of a small contribution of iron/titanium phases.

The results of the mineralogical analysis were supported by the SEM analysis. By the sequence reported

TABLE II Mechanical properties of the sintered glass-ceramic SC

Density ρ (g/cm^3)	2.85
Elastic modulus E (GPa)	100.62
Bending strength σ (MPa)	136.70 ± 9.21
Vickers' hardness H_V (GPa)	6.50 ± 0.64
Fracture toughness K_{IC} ($\text{MPa m}^{0.5}$)	2.29 ± 0.25

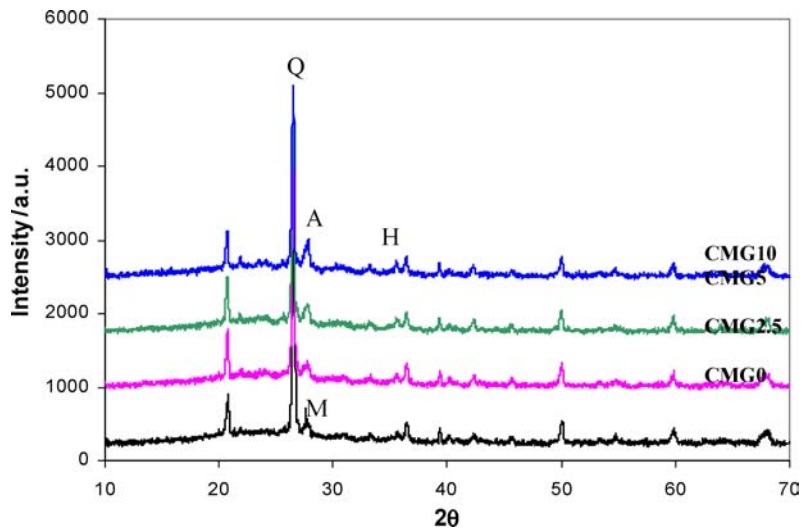


Figure 3 Comparison of XRD patterns of the SG frit containing samples fired in the industrial kiln.

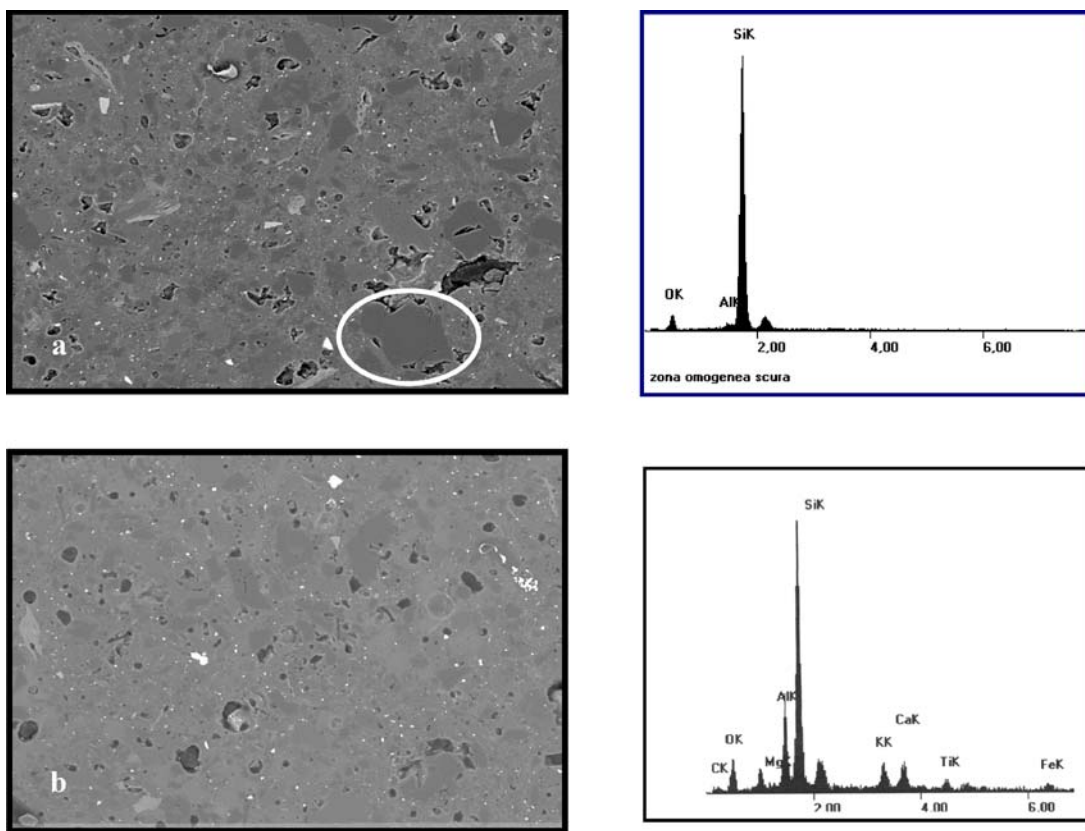


Figure 4 SEM micrographs (left, 160X) of (a) base body, (b) 10 wt% SG glass containing ceramics and EDS spectrum (right) of the signed zone in (c) the base body and (d) 10 wt% SG glass containing ceramics.

in Fig. 4 it appears evident that the increase of the frit percentage in the body decreases the quartz and porosity, and increases the samples sintering degree, the amorphous phase presence and the calcium rich zones. This is a direct consequence of the the anorthite phase formation, as detected by XRD analysis.

The photographs show that the pores having large dimensions and irregular shape (CMG0) become spherical and isolated from each other (CMG10); the CMG10 sample is more uniform with respect to the others probably due to the greater quantity of fluid phase with low viscosity during the firing.

The water absorption and linear shrinkage data are reported in Table III.

The experimentally obtained water absorption values, are lower than those typical of red single firing (WA < 3% [19, 21]) In every case the trend of the results indicates that the frit introduction into a ceramic

TABLE III WA% and LS% of the ceramic tiles

	CMG0	CMG2.5	CMG5	CMG10
WA%	0.36	0.33	0.20	0.21
LS%	8.25	8.50	8.38	8.25

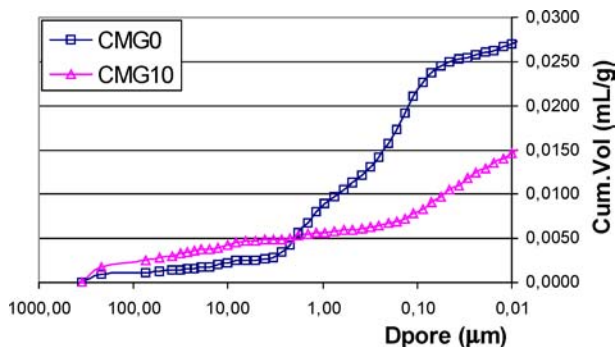


Figure 5 Semilog cumulative intrusion curves.

product determines a decrease in the water absorption values, notwithstanding a stabilization is observed starting from the addition of 5% of *G* frit. This trend is due to the presence of a glassy phase: it induces a liquid phase sintering process which favours the decrease of the open porosity. Concerning the linear shrinkage, the addition of *G* glass powders to a ceramic body does not substantially modify their characteristic values for single firing (which are around 8%).

A further confirmation of the positive effect of the (*G*) glass introduction on the porosity is pointed out by the mercury porosimetry measurements. This technique shows a porosity value for CMG0 of 7.17% and for CMG10 of 4.60%. In Fig. 5 are reported the intrusion cumulative curves (corresponding to the Hg volume change by increasing pressure) for CMG0 and CMG10. From the comparison of the curves it is evident that the corrected mixture has a more uniform pore distribution with respect to the base body, characterized by a bimodal distribution, because of a less Hg intruded volume. Moreover, 60% of the total porosity shows pore diameter lower than 0.15 μm .

As it is known, the Young's modulus and the bending strength are strictly related to inherent characteristics of materials, such as porosity, crystalline phases, and processing. Moreover, as emerged from the above reported results, it is evident that the introduction of a *G* frit into the ceramic mixtures improves the increase the compactness thanks to the presence of a low viscosity fluid phase during the firing, capable of filling the pores. As regards the Young's modulus *E* (Table IV), additions up to 5 wt% of *G* glass determine an *E* variation around 3.5%, while a 10% glass addition produces

TABLE IV Density (ρ), modulus of elasticity (*E*), flexural strength (σ_f) and Vickers' hardness with the relative percentage increments of the fired ceramic samples

	CMG0	CMG2.5	CMG5	CMG10
ρ (gr/cm ³)	2.24 ± 0.13	2.33 ± 0.04	2.34 ± 0.04	2.34 ± 0.09
$\Delta\rho$ (%)	0.00	4.02	4.46	4.46
<i>E</i> (GPa)	38.87	40.29	40.18	41.26
ΔE (%)	0.00	3.65	3.37	6.15
σ_f (MPa)	40.18 ± 1.94	43.24 ± 0.57	40.59 ± 2.28	40.79 ± 3.10
$\Delta\sigma_f$ (%)	0.00	7.62	1.02	1.52
<i>H_V</i> (GPa)	6.71 ± 1.22	5.08 ± 0.77	5.26 ± 0.67	6.03 ± 0.44
ΔH_V (%)	0.00	-24.29	-21.61	-10.13

a double increment. The flexural strength σ_f (Table IV) of all the samples remains practically constant and the values fall in the industrial requirement range of this category of product (30–40 MPa [19,21]).

The Vickers' microhardness is lowered by the addition of the *G* glass frit; there is a notable decrease for a low glass percentage (2.5%), while for further addition the hardness increases, becoming comparable to that of the ceramic body without any addition. This behaviour may be related from one hand to the decrease of the hard quartz phase and from the other to the increase of densification due to the formation, with the glass frit, of a fluid phase upon firing of the ceramic body.

4. Conclusions

The capability to recovery hazardous wastes as secondary raw material has been tested.

The obtained ceramic products exhibit promising physical and mechanical characteristics, which make them good candidates as useful materials in the construction field, such as tiles; the overall properties are better than those of traditional materials and could yield products with enhanced performances.

In fact, the glass-ceramic material shaped by sinter-crystallization of 80 parts of calcined spoils and 20 of glass cullet shows very good mechanical properties (in particular they show high bending strength and fracture toughness). Moreover, sinter-crystallization is resulted more effective with respect to bulk process to get a dense material by a relatively short thermal treatment.

Also the good results achieved for the ceramic samples, formulated between the vitrified spoils and the ceramic body, support the research in this field. In fact, the introduction of the glass residue determines an increase of the sintering degree together with a decrease of the total porosity of the obtained material. The mechanical properties are not practically modified and are upper than the industrial limits. Finally, for all the percentages investigated, the characteristics of the traditional productive cycle are not substantially altered, allowing a certain production economics.

References

1. P. COLOMBO, G. BRUSATIN, E. BERNARDO and G. SCARINCI, *Curr. Opin. Solid State Mater. Sci.* **7**(3) (2003) 225.
2. R. GUTMAN, *Glastech. Ber. Glass Sci. Technol.* **69**(9) (1996) 223.
3. E. J DE GUIRE and S. H. RISBUD, *J. Mat. Sci.* **19** (1984) 1760.
4. S. KLEMANTASKI, W. A. ARCHIBALD, S. SCHOLLES, A. P. SIKORSKI and P. S. ROGERS, *British Patent* 986289 (1965).
5. A. KARAMANOV, I. GUTZOW, I. CHOMAKOV, J. CHRISTOV and L. KOSTOV, *Glastech. Ber. Glass Sci. Technol.* **67**(8) (1994) 227.
6. A. KARAMANOV, M. PELINO and I. GUTZOW, in *Proc. XVIII Int. Cong. On Glass*, S. Francisco (1998).
7. C. CANTALE, S. CASTELLI, A. DONATO, D. M. TRAVERSO, P. COLOMBO and G. SCARINCI, *Rad. Waste Manag. Nucl. Fuel Cycle* **16** (1991) 25.
8. G. SCARINCI, G. BRUSATIN, L. BARBIERI, A. CORRADI, I. LANCELLOTTI, P. COLOMBO, S. HREGLICH and R. DALL'IGNA, *J. Eur. Ceram. Soc.* **20** (2000) 2485.

9. A. G. BERNSTEIN, E. BONSEMBIANTE, G. BRUSATIN, G. CALZOLARI, P. COLOMBO, R. DALL'IGNA, S. HREGLICH and G. SCARINCI, *Waste Management* **22**(8) (2002) 865.
10. G. BRUSATIN, A. G. BERNSTEIN, E. BONSEMBIANTE, G. CALZOLARI, P. COLOMBO, R. DALL'IGNA, S. HREGLICH and G. SCARINCI, in Proc. of the 6th World Congress on Integrated Resources Management, Geneva 12-15 Feb. 2002.
11. M. W. DAVIES, B. KERRISON, W. E. GROSS, M. J. ROBSON and D. F. WITCHALL, *J. Iron Steel Inst.* **208** (1973) 348.
12. P. D. SARKISOV, The Modern State of Technology and Application of Glass-Ceramics, in: Glass'89 Survey papers of the XVth International Congress on Glass Leningrad (1989) p. 411.
13. L. BARBIERI, A. CORRADI and I. LANCELOTTI, *J. Europ. Ceram. Soc.* **22**(11) (2002) 1759.
14. A. KARAMANOV, G. TAGLIERI and M. PELINO, *J. Am. Ceram. Soc.* **82** (1999) 3012.
15. I. GUTZOW, R. PASCOVA, A. KARAMANOV and J. SCHMELZER *J. Mater. Sci.* **33** (1998) 5265.
16. R. MÜLLER, E. D. ZANOTTO and V. M. FOKIN, *J. Non-Cryst. Sol.* **274** (2000) 208.
17. K. HERITAGE, C. FRISY and H. HOLFENDER, *Rev. Sci. Instru.* **59** (1988) 973.
18. G. R. ANSTIS, P. CHANTIKUL, B. R. LAWN and D. B. MARSHALL, *J. Amer. Ceram. Soc.* **64** (1981) 533.
19. G. P. EMILIANI and F. CORBARA, *Tecnologia Ceramica. Le Tipologie*. Gruppo Editoriale Faenza editrice s.p.a. Vol III, pp. 679-718.
20. L. BARBIERI, I. LANCELOTTI, T. MANFREDINI, I. QUERALT, J. MA. RINCÒN and M. ROMERO, *Fuel* **78** (1999) 271.
21. International Organisation for standardisation ISO13006.

*Received 12 August
and accepted 17 November 2004*